Stochastic theory of time-resolved four-wave mixing in interacting media

Stefan Schmitt-Rink and Shaul Mukamel*
AT&T Bell Laboratories, Murray Hill, New Jersey 07974

Karl Leo and Jagdeep Shah
AT&T Bell Laboratories, Holmdel, New Jersey 07733

Daniel S. Chemla
Lawerence Berkeley Laboratory and Department of Physics, University of California, Berkeley, California 94720
(Received 19 February 1991)

We study the temporal profile of the time-resolved four-wave-mixing signal in media with strong polarization interactions, assuming a stochastic modulation of the optical-transition frequency. The model is exactly solvable and interpolates smoothly between Lorentzian (fast modulation) and Gaussian (slow modulation) broadening. We show that recently predicted and observed four-wave-mixing signals persist even in the latter limit, albeit with a different temporal profile.

I. INTRODUCTION

Time-resolved four-wave-mixing (FWM) experiments provide a powerful tool for studying the dephasing of electronic excitations in crystals and molecular systems [1,2]. They are commonly interpreted via the nonlinear response function [3,4]. Simple theories for the latter usually make two general assumptions. (i) The local field acting at a particular site is taken to be equal to the externally applied field (or treated approximately by multiplying the nonlinear susceptibility with a local field correction factor) [5,6]. (ii) In real materials, the excitonic system is coupled to a bath of other degrees of freedom (phonons, solvent modes, etc.). The bath is assumed to be either very fast or very slow compared to the characteristic inverse exciton-bath coupling. The broadening of the linear absorption line shape in these two limits is usually denoted homogeneous and inhomogeneous, respectively; in many cases, the respective line shapes assume a Lorentzian or Gaussian form. Calculations where *either* assumption (i) or (ii) has been relaxed were carried out in the past. For example, Bloch-like equations of motion which incorporate local field corrections have been used to relax approximation (i) [7]. Approximation (ii) may be relaxed by using a stochastic model for the bath with an arbitrary time scale [8]. The nonlinear response function for this model has been determined exactly and applied to a variety of FWM techniques, such as CARS and photon echo [4,9]. More recently, these calculations have been generalized to a Brownian oscillator model for the bath [4,10].

In this paper, we develop an expression for the nonlinear response function in which *both* of the above approximations are relaxed. For clarity, we limit ourselves to the simplest FWM geometry, in which two laser pulses centered at times $t_1=-T$ and $t_2=0$ and propagating in the directions $\mathbf{k}_1$ and $\mathbf{k}_2$ interfere in a sample to generate a transient grating which diffracts photons into the direction $\mathbf{k}_s=2\mathbf{k}_2-\mathbf{k}_1$ (see inset to Fig. 4). The pulses are assumed to be very short compared to any relaxation time of the system (but not compared to the optical frequency) [11]. Recently, the FWM signal for this situation has been calculated by relaxing approximation (i), but assuming a very short bath time scale so that a Bloch-like description becomes valid [12]. It was found that the local field corrections result in a new component to the FWM signal which was subsequently observed in semiconductors [12,13]. In this article, we extent the theory to the case of a bath with an arbitrary time scale and further explore the physical origin and characteristics of this novel signal.

II. THE NONLINEAR RESPONSE FUNCTION

Our starting point is the polarization written in terms of the dipole matrix element μ and the average of the exciton amplitude ψ over the bath

$$P(t)=\mu^*\langle\psi(t)\rangle\ . \tag{1}$$

For a variety of systems, including molecular crystals and semiconductors, it may be shown that ψ satisfies a nonlinear Schrödinger equation of the form [12,14,15]

$$\frac{\partial}{\partial t}\psi(t)=-i[\omega(t)-i\Gamma]\psi(t) +i\mu E(t)\left[1-\frac{|\psi(t)|^2}{|\psi_s|^2}\right]-iV|\psi'(t)|^2\psi(t)\ , \tag{2}$$

where only terms up to third order in the applied field E have been considered. Let us comment on the physical meaning of the various terms in Eq. (2). Γ is the exciton half-width at half maximum (HWHM) due to radiative decay and $\omega(t)=\omega_0+\delta\omega(t)$ is the exciton energy which we assume to be stochastically modulated. Here, ω_0 is

the energy of an isolated exciton and $\delta\omega(t)$, $\langle\delta\omega(t)\rangle=0$, is a time-dependent modulation imposed by the bath. The second (two-level-like) term $i\mu E(t)[1-|\psi(t)|^2/|\psi_s|^2]$ describes the dipole coupling of excitons to the applied field, including the effects of Pauli exclusion. $|\psi_s|^2$ is the saturation density which depends on the exciton parameters [14,15] and in the simple case of two-level systems reduces to $\frac{1}{2}$. The third (anharmonic-oscillator-like) term $-iV|\psi'(t)|^2\psi(t)$ describes exciton-exciton interactions or nonlinear local field corrections. Its physical interpretation is that excitons $\psi(t)$ interact via V with excitons at different sites, $\psi'(t)$. The latter satisfy a similar equation, with $\delta\omega(t)$ replaced by $\delta\omega'(t)$. This term makes Eq. (2) nonlocal in space and introduces an unusual time dependence of the nonlinear polarization, since for ultrashort applied fields $E(t)\sim\delta(t)$, $\psi(t)$ and $\psi'(t)$ exhibit steplike behavior $\sim\Theta(t)$. We note that in semiconductors the polarization interaction energy V is real and positive, resulting in a density-dependent exciton blue shift in pump-probe experiments [16], while in molecular crystals V is determined by the linear dielectric properties of the medium.

Equation (2) may be solved by expanding ψ in powers of the applied field E. We obtain for the first- and third-order terms

$$\psi^{(1)}(t)=i\mu\int_{-\infty}^{t}dt'\exp\left[-i\int_{t'}^{t}d\tau\,\omega(\tau)-\Gamma(t-t')\right]E(t') \tag{3}$$

and

$$\psi^{(3)}(t)=-\frac{i\mu}{|\psi_s|^2}\int_{-\infty}^{t}dt'\exp\left[-i\int_{t'}^{t}d\tau\,\omega(\tau)-\Gamma(t-t')\right]\times\left[|\psi^{(1)}(t')|^2E(t')+\frac{V|\psi_s|^2}{\mu}|\psi'^{(1)}(t')|^2\psi^{(1)}(t')\right], \tag{4}$$

which generalizes the Bloch equation results of Ref. [12] to the case of a time-dependent exciton energy.

Equation (4) shows that in the presence of polarization interactions there are two distinct physical processes contributing to the FWM signal, (i) scattering of an induced polarization off the transient grating (second term in the second set of large parentheses) and (ii) scattering of the applied field itself (first term in the second set of large parentheses) [12,13]. More precisely, in a FWM experiment the first pulse induces a polarization that subsequently undergoes free induction decay, i.e., continues to radiate, for a time determined by the dephasing. When the second pulse arrives, it also induces a polarization. This second polarization creates by interference with the remaining first polarization a transient grating that scatters both the second pulse field *and* the ongoing free induction decay radiation.

Substituting $E(t)=E_1\delta(t+T)\exp(i\mathbf{k}_1\mathbf{r})+E_2\delta(t)\times\exp(i\mathbf{k}_2\mathbf{r})$ into Eqs. (3) and (4) and using the rotating-wave approximation, we obtain three contributions to the induced polarization in the direction $\mathbf{k}_s=2\mathbf{k}_2-\mathbf{k}_1$ which may be written in a time-ordered fashion. Two cases may be distinguished: In case 1 pulse no. 1 acts first (at time $-T$) and pulse no. 2 acts second (at time 0). In case 2 pulse no. 2 acts first (at time 0) and pulse no. 1 acts second (at time $-T$). The delay T between the two pulses is therefore positive in case 1 and negative in case 2.

In case 1 ($T>0$) the third-order polarization $P^{(3)}_{\mathbf{k}_s}$ is finite for all $t>0$ and consists of two terms

$$P^{(3)}_{\mathbf{k}_s}(t)=\kappa e^{-i\omega_0(t-T)-\Gamma(t+T)}\times\left[A_0+A_V i2V|\psi_s|^2\frac{1-e^{-2\Gamma t}}{2\Gamma}\right]. \tag{5a}$$

In case 2 ($T<0$) $P^{(3)}_{\mathbf{k}_s}$ is finite for all $t>-T$ and consists of one term

$$P^{(3)}_{\mathbf{k}_s}(t)=\kappa e^{-i\omega_0(t-T)-\Gamma(t+T)}\times\left[A_V i2V|\Psi_s|^2\frac{e^{2\Gamma t}-e^{-2\Gamma t}}{2\Gamma}\right], \tag{5b}$$

where $\kappa\equiv-i|\mu|^4E_2^2E_1^*/2|\psi_s|^2$. Finally, the FWM signal is given by

$$I_{\mathbf{k}_s}\propto\int_{-\infty}^{\infty}dt|P^{(3)}_{\mathbf{k}_s}(t)|^2. \tag{6}$$

The third-order polarization Eqs. (5) is determined by the amplitudes A_0 and A_V. The time-ordered expressions for these amplitudes read

$$A_0=\left\langle\exp\left[-i\int_0^t d\tau\,\delta\omega(\tau)+i\int_{-T}^0 d\tau\,\delta\omega(\tau)\right]\right\rangle \tag{7a}$$

and

$$A_V=\left\langle\exp\left[-i\int_0^t d\tau\,\delta\omega(\tau)+i\int_{-T}^0 d\tau\,\delta\omega'(\tau)\right]\right\rangle \tag{7b}$$

$$=\left\langle\exp\left[-i\int_{-T}^t d\tau\,\delta\omega(\tau)-i\int_0^{-T}d\tau[\delta\omega(\tau)+\delta\omega'(\tau)]\right]\right\rangle. \tag{7c}$$

A_0 represents the single-site contribution to the signal; it is always present, even in the absence of polarization interactions, $V=0$. It describes the modulation of the exciton energy by the bath at a given site, i.e., it involves only $\delta\omega$. A_V represents the interaction-induced intersite contribution. It involves the modulation of the exciton energy by the bath at two different sites ($\delta\omega$ and $\delta\omega'$) and is mediated by V; i.e., the A_V term is absent if we set $V=0$. The explicit form of A_0 and A_V depends of course on the details of the exciton-bath interaction (see below).

The physical origin of the phase factors in Eqs. (7) can be visualized using the double-sided Feynman diagrams

shown in Fig. 1. They describe the dephasing of the density matrix $\hat{\rho}$ during time intervals of free evolution between interactions with the various fields. For case 1 we have both a single-site and interaction-induced intersite contribution. They are displayed in Figs. 1(a) and 1(b), respectively. Diagram 1(a) is the common physical picture of the ordinary photon echo [4,10]. The first pulse ($\mathbf{k}_1$) brings the density matrix from the ground state ρ_{gg} to an optical coherence ρ_{ge}. The second pulse ($\mathbf{k}_2$) interacts twice and changes the density matrix to ρ_{eg} [Eq. (7a)]. Diagram 1(b) represents the interaction-induced intersite term. The first pulse ($\mathbf{k}_1$) as in 1(a) creates an optical coherence ρ_{eg} at the second site. The second pulse ($\mathbf{k}_2$) interacts once with each site. It brings the second site back to the ground state ρ_{gg} and the first site to ρ_{eg} [Eq. (7b)]. For case 2 we have only one diagram, 1(c). Here, the first pulse ($\mathbf{k}_2$) creates an optical coherence ρ_{eg} at both sites so that during the first temporal evolution period we have two phase factors. The second pulse ($\mathbf{k}_1$) brings the second site back to the ground state ρ_{gg} so that during the second temporal evolution period only the first site is in an optical coherence ρ_{eg} [Eq. (7c)]. In all cases, radiation of the signal ($\mathbf{k}_s$) finally brings the system back to the ground state ρ_{gg}.

The temporal evolution of A_V depends on the model we adopt for the correlation among frequency fluctuations at different sites. We define the single-site correlation function for the frequency fluctuations

$$\langle \delta\omega(\tau)\delta\omega(0)\rangle \equiv M(\tau) \tag{8}$$

and write the two-site correlation function as

$$\langle \delta\omega(\tau)\delta\omega'(0)\rangle = \eta M(\tau)\ , \tag{9}$$

where η is an intersite correlation factor ($\eta=0$: no correlation; $\eta=1$: full correlation). The average over the stochastic variables invoked in the calculation of A_0 and A_V may now be carried out formally by expanding expressions (7) to second order in $\delta\omega$, time-ordering the resulting integrals, and identifying them with a second-order cumulant expansion [9]. We obtain

$$A_0 = e^{-2g(t)-2g(T)+g(t+T)} \tag{10a}$$

and

$$A_V = e^{-(1+\eta)g(t)-(1+\eta)g(T)+\eta g(t+T)}\ , \tag{10b}$$

where

$$g(t) = \int_0^t d\tau_1 \int_0^{\tau_1} d\tau_2 M(\tau_2)\ . \tag{11}$$

In the case of full intersite correlation, $\eta=1$, we have $A_0 = A_V$. For completeness we note that the linear absorption line shape for this model is given by [4,8]

$$\mathrm{Im}\chi(\omega) = |\mu|^2 \mathrm{Re}\int_0^\infty dt\, e^{i(\omega-\omega_0+i\Gamma)t-g(t)}\ . \tag{12}$$

To gain further insight into the different nature of the single-site and interaction-induced intersite terms, let us consider $\Gamma=0$ and the two limiting cases of (i) very short and (ii) very long bath time scale. In case (i) we can write

$$M(\tau) = D^2\delta\left[\frac{\tau}{T_c}\right]\ , \tag{13a}$$

where D is the exciton-bath coupling and T_c is a characteristic (very short) bath correlation time. Introducing the transverse exciton relaxation time $T_2 = (D^2 T_c)^{-1}$, we then have

$$g(t) = \frac{|t|}{T_2} \tag{13b}$$

and

$$\mathrm{Im}\chi(\omega) = \frac{|\mu|^2 T_2^{-1}}{(\omega-\omega_0)^2 + T_2^{-2}}\ . \tag{13c}$$

In case (ii) we can write

$$M(\tau) = D^2\ , \tag{14a}$$

which yields

$$g(t) = \tfrac{1}{2}D^2 t^2 \tag{14b}$$

and

$$\mathrm{Im}\chi(\omega) = \frac{|\mu|^2\sqrt{\pi}}{D\sqrt{2}} e^{-(\omega-\omega_0)^2/2D^2}\ . \tag{14c}$$

Equations (13c) and (14c) correspond to the well-known

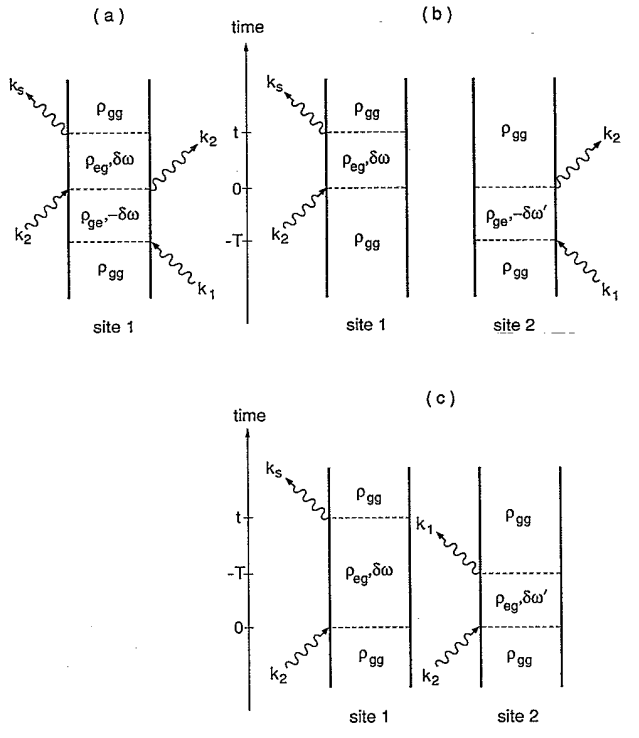

FIG. 1. Double-sided Feynman diagrams for four-wave mixing in interacting media. (a) is the single-site contribution, (b) and (c) are the interaction-induced intersite contributions. Time runs from the bottom to the top and wavy arrows denote interactions with the applied field. ρ is the density matrix. Also shown are the phase factors $\delta\omega$ and $\delta\omega'$ associated with each time interval.

limiting cases of homogeneous (Lorentzian) and inhomogeneous (Gaussian) broadening, respectively [4,8].

Consider now a system with two independent broadening mechanisms, one homogeneous and the other inhomogeneous. For this model we have $g=g_1+g_2$, where g_1 is given by Eq. (13b) and g_2 by Eq. (14b). Substituting these expressions into Eqs. (10), we obtain

$$A_0=e^{-D^2(t-T)^2/2+(t+T)/T_2} \tag{15a}$$

and

$$A_V=e^{-D^2(t^2-2\eta tT+T^2)/2-[t+(1+\eta)|T|-\eta T]/T_2} . \tag{15b}$$

We note that for large inhomogeneous broadening the single-site term A_0 is sharply peaked at $t=T$. This peak is called photon echo. It originates from the exact cancellation of the phases acquired by ρ_{ge} and ρ_{eg} during the consecutive two periods of temporal evolution [Fig. 1(a)]. This is clearly seen in Eq. (7a) which shows that the frequency fluctuations during the $(0,t)$ and $(-T,0)$ time intervals appear in A_0 with opposite signs. For a static distribution [$\delta\omega(t)$ independent of t], the two phase factors cancel exactly. The interaction-induced intersite term A_V shown in Fig. 1(c), on the other hand, does not give rise to a photon echo, because the phases never cancel. According to Eq. (7c), during the $(-T,t)$ time interval we have the frequency fluctuation $\delta\omega$ whereas during the $(0,-T)$ time interval we have $\delta\omega+\delta\omega'$. The phase factors for both time intervals appear with the same sign and they never cancel. This term is particularly interesting, since it is the only contribution for $T<0$. It thus provides a direct and background-free manifestation of interactions. Finally, the A_V term shown in Fig. 1(b) gives rise to a photon echo only when the sites are fully correlated ($\eta=1$). Being only a correction to the A_0 term, its effects are less distinct.

III. NUMERICAL RESULTS AND DISCUSSION

In order to illustrate the continuous transition from homogeneous to inhomogeneous broadening, we adopt the following well-known form of the correlation function [8]:

$$M(\tau)=D^2e^{-|t|/T_c} . \tag{16a}$$

Substituting Eq. (16a) into Eq. (11) yields

$$g(t)=-(DT_c)^2\left[1-\frac{|t|}{T_c}-e^{-|t|/T_c}\right] , \tag{16b}$$

which reproduces Eqs. (13b) and (14b) for $DT_c\ll1$ and $DT_c\gg1$, respectively. Neglecting radiative lifetime effects ($\Gamma=0$), a simple Padé approximant for the full width at half maximum (FWHM) 2γ of the linear absorption Eq. (12) is [17]

$$2\gamma=D\frac{2(DT_c)+2.676(DT_c)^2}{1+0.966(DT_c)+1.136(DT_c)^2} . \tag{17}$$

This expression is accurate to within a few percent. In the following, we use $(2\gamma)^{-1}$ as the (fixed) unit of time

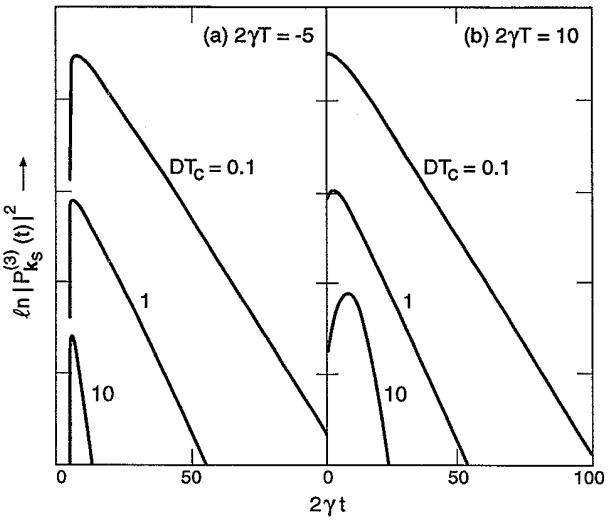

FIG. 2. Time-resolved four-wave-mixing signal $|P^{(3)}_{k_s}(t)|^2$ for different time delays T and line-shape parameters DT_c.

and vary DT_c. In other words, we consider a series of linear absorption line shapes with the same FWHM 2γ and vary the parameter DT_c, thus changing the character of the line shape from homogeneous to inhomogeneous. For $DT_c\ll1$ the linear absorption line shape is a Lorentzian of width 2γ, for $DT_c\gg1$ it is a Gaussian of width 2γ. Also, to make contact with the earlier work on the problem [12], we only consider the case of uncorrelated sites, $\eta=0$.

Figure 2 shows the time-resolved FWM signal, i.e., the integrand $|P^{(3)}_{k_s}(t)|^2$ in Eq. (6), for $V^2|\psi_s|^4=\gamma^2$, different time delays T and line-shape parameters DT_c. In Fig. 2(a) the time delay T is negative and in Fig. 2(b) it is positive. In the homogeneous limit $DT_c\ll1$ and for $T<0$ ($T>0$) the signal begins immediately after the second pulse, $t>-T$ ($t>0$), and subsequently decays exponentially with the FWHM, 2γ. For $T<0$, as DT_c increases toward the inhomogeneous limit $DT_c\gg1$, the decay at long times becomes faster. However, the signal still begins at $t=-T$. For $T>0$, on the other hand, the signal peak moves toward $t=T$, i.e., we obtain a photon echo. This photon echo is due to the single-site contribution. In fact, the results for $T>0$ look essentially the same in the absence of polarization interactions, $V=0$ [11]. Of course, the $T<0$ signal would then also be absent.

Figure 3 shows the time-integrated FWM signal Eq. (6) versus time delay T for the same line-shape parameters DT_c as in Fig. 2. In the homogeneous limit $DT_c\ll1$ and for $T<0$ the signal rises exponentially with twice the FWHM, 4γ, while for $T>0$ it decays with the FWHM, 2γ. This is the result found previously from Bloch equations including local field corrections [12]. As DT_c increases toward the inhomogeneous limit $DT_c\gg1$, the rise and decay become faster and the signal for $|T|\ll T_c$ becomes suppressed. However, for time delays much longer than the correlation time, $|T|\gg T_c$, the rise and decay remain exponential, with time constants of $T_2/4$

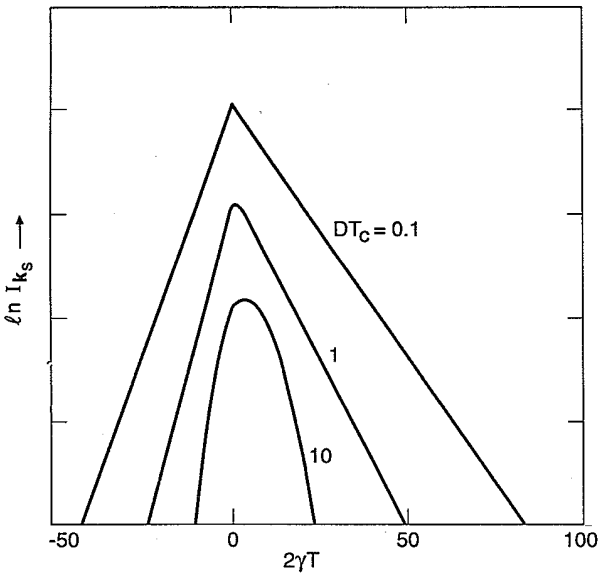

FIG. 3. Time-integrated four-wave-mixing signal I_{k_s} vs time delay T for different line-shape parameters DT_c.

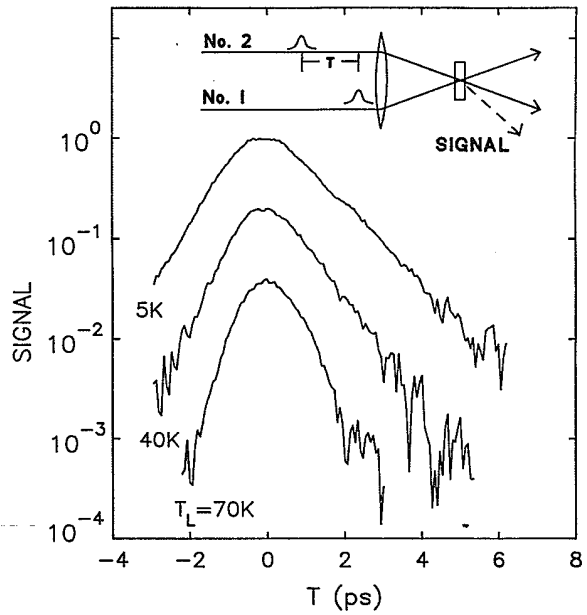

FIG. 4. Experimental time-integrated four-wave-mixing signal in GaAs/$Ga_{1-x}Al_xAs$ vs time delay T for different lattice temperatures T_L, taken with 500-fs laser pulses. The inset shows the geometry of the experiment.

and $T_2/2$, respectively. In this limit, the dephasing is thus always Markovian and the description in terms of Bloch equations remains valid.

Figure 4 shows experimental time-integrated FWM signals in GaAs/$Al_{1-x}Ga_xAs$ versus time delay T for different lattice temperatures T_L, taken with 500-fs laser pulses [13]. The sample is a high-quality 170-Å multiple-quantum-well structure, with the substrate removed to allow transmission experiments. In qualitative agreement with theory (Fig. 3), the signals are asymmetric in time, with exponentially rising and decaying wings at long time delays. As the lattice temperature is raised, both the decay and the rise time get shorter, due to increasing dephasing of the excitons by thermal phonons.

At the lowest temperature $T_L = 5$ K, the ratio of decay and rise time constants is within the experimental error equal to 2:1, as predicted by theory. Furthermore, the signal is exponential for all $|T|$ larger than the pulse duration which therefore must be longer than the bath correlation time. At higher temperatures, the time resolution of the experiments hinders a quantitative analysis.

For simplicity, we have used in our numerical calculations the simple stochastic model Eq. (16). Especially for solvated molecules, a more general microscopic model is to assume that the bath can be represented by a collection of independent harmonic oscillators undergoing Brownian motion [4,10]. We thus write

$$\delta\omega(t)=\sum_j D_j q_j(t) \ . \tag{18a}$$

q_j is a dimensionless oscillator coordinate which we assume to obey the Langevin equation

$$\frac{\partial^2}{\partial t^2}q_j(t)+\gamma_j\frac{\partial}{\partial t}q_j(t)+\omega_j^2 q_j(t)=f_j(t) \ , \tag{18b}$$

where f_j is a random Langevin force and γ_j is the associated friction, related to f_j by the fluctuation-dissipation theorem

$$\langle f_j(t)f_k(0)\rangle=\frac{2\gamma_j k_B T}{\omega_j}\delta_{jk}\delta(t) \ . \tag{18c}$$

The real part of the resulting line-shape function g may be written as

$$\mathrm{Re}g(t)=\frac{1}{2\pi}\int_{-\infty}^{\infty}d\omega\frac{1-\cos\omega t}{\omega^2}C(\omega) \ , \tag{18d}$$

where

$$C(\omega)=\sum_j\frac{2\Delta_j^2\omega_j^2\gamma_j}{(\omega^2-\omega_j^2)^2+(\omega\gamma_j)^2} \tag{18e}$$

is the spectral density of bath excitations and $\Delta_j^2=D_j^2 k_B T/\omega_j$. For $\gamma_j \ll \omega_j$ the oscillators are underdamped and Reg exhibits coherent oscillations with frequencies ω_j. For $\gamma_j \gg \omega_j$ the oscillators are overdamped and the model reduces to the stochastic model Eq. (16) with $T_c=\gamma_j/\omega_j^2$.

We note that the full line-shape function g for the mod-

el Eqs. (18) is complex. Its imaginary part describes the time-dependent Stokes shift [4,10]. The resulting nonlinear response function for FWM in the absence of polarization interactions was discussed previously. It was found that apart from an overall (and hence irrelevant) phase factor, Eq. (10a) remains valid, with g replaced by Reg [4,10]. Thus all our formal results may be also applied to this more realistic model. As for delocalized excitons in semiconductors, they are only approximately described by a second-order cumulant expansion [18]. We hope to present corresponding FWM profiles in the near future.

ACKNOWLEDGMENTS

Part of this work was performed while S. M. was visiting AT&T Bell Laboratories. He wishes to thank the technical staff for their hospitality. The work of S.M. was supported by the National Science Foundation, the Air Force Office of Scientific Research, and the Petroleum Research Fund, administered by the American Chemical Society. The work of D.S.C. was supported by the Director, Office of Energy Research—Office of Basic Energy Sciences, Materials Sciences Division of the Department of Energy.

*Permanent address: Department of Chemistry, University of Rochester, Rochester, NY 14627.

[1] For recent experiments on localized excitations in molecular systems, see, e.g., P. C. Becker, H. L. Fragnito, J. Y. Bigot, C. H. Brito Cruz, R. L. Fork, and C. V. Shank, Phys. Rev. Lett. **63**, 505 (1989); J. Y. Bigot, M. T. Portella, R. W. Schoenlein, C. J. Bardeen, A. Migus, and C. V. Shank, *ibid.* **66**, 1138 (1991).

[2] For recent experiments on extended excitations in semiconductors, see, e.g., L. Schultheis, J. Kuhl, A. Honold, and C. W. Tu, Phys. Rev. Lett. **57**, 1635 (1986); **57**, 1797 (1986); P. C. Becker, H. L. Fragnito, C. H. Brito Cruz, R. L. Fork, J. E. Cunningham, J. E. Henry, and C. V. Shank, *ibid.* **61**, 1647 (1988); E. O. Goebel, K. Leo, T. C. Damen, J. Shah, S. Schmitt-Rink, W. Schaefer, J. F. Mueller, and K. Koehler, *ibid.* **64**, 1801 (1990); K. Leo, T. C. Damen, J. Shah, E. O. Goebel, and K. Koehler, Appl. Phys. Lett. **57**, 19 (1990); B. F. Feuerbacher, J. Kuhl, R. Eccleston, and K. Ploog, Solid State Commun. **74**, 1279 (1990); K. Leo, J. Shah, E. O. Goebel, T. C. Damen, S. Schmitt-Rink, W. Schaefer, and K. Koehler, Phys. Rev. Lett. **66**, 201 (1991).

[3] R. W. Hellwarth, Prog. Quantum Electron. **5**, 1 (1977); P. N. Butcher, *Nonlinear Optical Phenomena* (Ohio University Press, Athens, Ohio, 1965); T. Yajima and Y. Taira, J. Phys. Soc. Jpn. **47**, 1620 (1979).

[4] S. Mukamel, Adv. Chem. Phys. **70**, 165 (1988); Annu. Rev. Phys. Chem. **41**, 647 (1990).

[5] D. Bedeaux and N. Bloembergen, Physica **69**, 67 (1973).

[6] Y. R. Shen, *The Principles of Nonlinear Optics* (Wiley, New York, 1984).

[7] S. Mukamel, Z Deng, and J. Grad. J. Opt. Soc. Am. B **5**, 804 (1988); J. Knoester and S. Mukamel, Phys. Rev. A **39**, 1899 (1988).

[8] N. Bloembergen, E. M. Purcell, and R. V. Pound, Phys. Rev. **73**, 679 (1948); P. W. Anderson and P. R. Weiss, Rev. Mod. Phys. **25**, 269 (1953); R. Kubo, in *Fluctuations, Relaxation and Resonance in Magnetic Systems,* edited by D. ter Haar (Plenum, New York, 1962), p. 23.

[9] S. Mukamel, Phys. Rev. A **28**, 3480 (1983).

[10] Y. J. Yan and S. Mukamel, J. Chem. Phys. **94**, 179 (1991); W. B. Bosma, Y. J. Yan, and S. Mukamel, Phys. Rev. A **42**, 6920 (1990).

[11] R. F. Loring and S. Mukamel, Chem. Phys. Lett. **114**, 426 (1985).

[12] M. Wegener, D. S. Chemla, S. Schmitt-Rink, and W. Schaefer, Phys. Rev. A **42**, 5675 (1990); C. Stafford, S. Schmitt-Rink, and W. Schaefer, Phys. Rev. B **41**, 10 000 (1990).

[13] K. Leo, M. Wegener, J. Shah, D. S. Chemla, E. O. Goebel, T. C. Damen, S. Schmitt-Rink, and W. Schaefer, Phys. Rev. Lett. **65**, 1340 (1990).

[14] S. Schmitt-Rink, D. S. Chemla, and D. A. B. Miller, Phys. Rev. B **32**, 6601 (1985); S. Schmitt-Rink and D. S. Chemla, Phys. Rev. Lett. **57**, 2752 (1986); S. Schmitt-Rink, D. S. Chemla, and H. Haug, Phys. Rev. B **37**, 941 (1988).

[15] J. R. Kuklinski and S. Mukamel, Phys. Rev. B **42**, 2959 (1990); **42**, 11 938 (1990).

[16] N. Peyghambarian, H. M. Gibbs, J. L. Jewell, A. Antonetti, A. Migus, D. Hulin, and A. Mysyrowicz, Phys. Rev. Lett. **53**, 2433 (1984); J. B. Stark, W. H. Knox, D. S. Chemla, W. Schaefer, S. Schmitt-Rink, and C. Stafford, *ibid.* **65**, 3033 (1990).

[17] W. B. Bosma, Y. J. Yan, and S. Mukamel, J. Chem. Phys. **93**, 3863 (1990).

[18] J. Liebler, S. Schmitt-Rink, and H. Haug, J. Lumin. **34**, 1 (1985); J. Liebler and H. Haug, Europhys. Lett. **14**, 71 (1991).